

Provided for non-commercial research and education use.  
Not for reproduction, distribution or commercial use.



This article appeared in a journal published by Elsevier. The attached copy is furnished to the author for internal non-commercial research and education use, including for instruction at the authors institution and sharing with colleagues.

Other uses, including reproduction and distribution, or selling or licensing copies, or posting to personal, institutional or third party websites are prohibited.

In most cases authors are permitted to post their version of the article (e.g. in Word or Tex form) to their personal website or institutional repository. Authors requiring further information regarding Elsevier's archiving and manuscript policies are encouraged to visit:

<http://www.elsevier.com/copyright>



Contents lists available at ScienceDirect

## Separation and Purification Technology

journal homepage: [www.elsevier.com/locate/seppur](http://www.elsevier.com/locate/seppur)

## Flue gas desulphurization based on limestone-gypsum with a novel wet-type PCF device

Hongliang Gao<sup>a,b</sup>, Caiting Li<sup>a,b,\*</sup>, Guangming Zeng<sup>a,b</sup>, Wei Zhang<sup>a,b</sup>, Lin Shi<sup>a,b</sup>, Shanhong Li<sup>a,b</sup>, Yanan Zeng<sup>c</sup>, Xiaopeng Fan<sup>a,b</sup>, Qingbo Wen<sup>a,b</sup>, Xin Shu<sup>a,b</sup>

<sup>a</sup> College of Environmental Science and Engineering, Hunan University, Changsha 410082, PR China

<sup>b</sup> Key Laboratory of Environmental Biology and Pollution Control (Hunan University), Ministry of Education, Changsha 410082, PR China

<sup>c</sup> College of Economics, Central South University of Forestry and Technology, Changsha 410004, PR China

### ARTICLE INFO

#### Article history:

Received 22 May 2010

Received in revised form 15 October 2010

Accepted 18 October 2010

#### Keywords:

Wet flue gas desulphurization

PCF device

Slurry

Absorption

Efficiency

### ABSTRACT

The wet flue gas desulphurization has been the most widely used in the coal-fired power plants because of high SO<sub>2</sub> removal efficiency, reliability and low utility consumption. In this paper, laboratory studies on the removal of SO<sub>2</sub> from gas mixtures with a novel wet-type PCF device (Chinese LOGO) were reported, CaCO<sub>3</sub>-in-water suspension used as absorbent. The main work included the influences of some process parameters such as slurry pH, limestone concentration in feed stream, SO<sub>2</sub> inlet concentration, liquid-gas ratio and superficial gas velocity. Meanwhile, the desulphurization process in the PCF device was analyzed using the two-film theory of gas-liquid mass-transfer. The results show that the PCF device has low pressure drop, large specific capacity for flue gas treatment, high absorption rate and good dewatering performance. Under moderate conditions, the concentration of SO<sub>2</sub> in outlet flue gas can achieve a much lower level than that of permitted. The reasonable operating conditions for the PCF device are as follows: slurry pH value is 5.7 ± 0.1, limestone concentration in feed stream is 13 wt.%, SO<sub>2</sub> inlet concentration is less than 4.1 g/m<sup>3</sup>, liquid-gas ratio is 8.7–10.4 L/m<sup>3</sup> and superficial gas velocity in preliminary treating chamber is 2.0–2.5 m/s (3.4–4.3 m/s in inner cylinder). Furthermore, the results obtained from the two-film theory show that the SO<sub>2</sub> removal rate is controlled by the combination of both gas- and liquid-film diffusions in the range of operating conditions tested.

© 2010 Elsevier B.V. All rights reserved.

### 1. Introduction

Combustion of sulphur-containing fossil fuels such as coal and oil results in sulphur dioxide (SO<sub>2</sub>) emission. SO<sub>2</sub> is known to have detrimental effects on human health and environment, and as a consequence, receives more and more attention [1]. Presently, there are several ways of reducing SO<sub>2</sub> emissions from coal utilization, such as fuel pretreatment, concurrent burning and adsorption, and flue gas post treatment, that is, flue gas desulphurization (FGD) [2,3]. Among those schemes, FGD is the most reasonable one from both technological and economic point of views, which leads it to be the most practically applicable. Different categories of processes, such as dry-, semidry- and wet-processes, have been developed for FGD. Among them, wet-processes, especially the limestone-gypsum process, have earned widespread use

due to high SO<sub>2</sub> removal efficiency, reliability and low utility consumption [4–6].

Since the goal of FGD is only for environmental protection and there are no value-added products during the course, research and development of the FGD technology has been focusing on improving the removal efficiency, minimizing water and energy consumptions [5]. The PCF device (Chinese LOGO) is newly developed for industrial application of wet FGD, having sleeve structure. It is derived from the conventional granite water film dust collector (GWFDC) by building an outer cylinder around the original GWFDC. The outer cylinder is lower than inner cylinder (original GWFDC), and between them is a preliminary treating chamber where gas and liquid contact and are in coflows. Self-excitation channels lying in the wall of the inner cylinder are employed to connect the preliminary treating chamber and inner cylinder and to simultaneously make the gas rotate into the inner cylinder. At the bottom of the inner cylinder is a self-excitation chamber that has second purification for the flue gas. The whole inner cylinder is used to remove water from air. Compared with the original GWFDC, the novel wet-type PCF device possesses the following virtues: (a) Dewatering performance improves significantly, and an extra demister is out of consideration. No demister means lower energy-consumption,

\* Corresponding author at: College of Environmental Science and Engineering, Hunan University, Changsha 410082, PR China.

Tel.: +86 731 88649216; fax: +86 731 88822829.

E-mail addresses: [ghliang007@163.com](mailto:ghliang007@163.com) (H. Gao), [ctli3@yahoo.com](mailto:ctli3@yahoo.com), [ctli@hnu.cn](mailto:ctli@hnu.cn) (C. Li).

**Nomenclature**

$a$	gas–liquid interface area ( $m^2$ )
$c_{CaCO_3}$	concentration of limestone in liquid phase ( $mol/m^3$ )
$c_{in}$	$SO_2$ inlet concentration ( $g/m^3$ )
$c_{out}$	$SO_2$ outlet concentration ( $g/m^3$ )
$c_{SO_2}$	concentration of $SO_2$ in liquid phase ( $mol/m^3$ )
$c_{SO_2}^*$	equilibrium concentration of $SO_2$ in liquid phase ( $mol/m^3$ )
$d_p$	average size of slurry droplets (m)
$D_{CaCO_3}$	calcium carbonate diffusion coefficient ( $m^2/s$ )
$D_G$	diffusion coefficient of $SO_2$ in gas phase ( $m^2/s$ )
$D_L$	diffusion coefficient of $SO_2$ in liquid phase ( $m^2/s$ )
$E$	mass-transfer enhancement factor (dimensionless)
$H_{SO_2}$	Henry's constant of $SO_2$ ( $mol/(m^3 Pa)$ )
$k_2$	equilibrium constant of Eq. (9)
$k_3$	equilibrium constant of Eq. (10)
$k_G$	gas-side mass-transfer coefficient ( $mol/(m^2 s Pa)$ )
$k_L$	liquid-side mass-transfer coefficient (m/s)
$K_G$	total mass-transfer coefficient ( $mol/(m^2 s Pa)$ )
$M_M$	molar mass of the liquid phase (g/mol)
$m_p$	mass of a droplet (kg)
$N_{SO_2}$	absorption rate of $SO_2$ (mol/s)
$P$	atmospheric pressure (Pa)
$\Delta p$	pressure drop (Pa)
$P_{Bm}$	logarithmically averaged pressure of interface and gas-phase of inert component (Pa)
$p_{SO_2}$	partial pressure of $SO_2$ in gas phase (Pa)
$p_{SO_2,avg}$	logarithmically averaged pressure of inlet and outlet (Pa)
$P_T$	overall pressure (Pa)
$p_{SO_2,in}$	partial pressure of $SO_2$ in gas phase at inlet (Pa)
$p_{SO_2,out}$	partial pressure of $SO_2$ in gas phase at outlet (Pa)
$\Delta p_{SO_2}$	absorption driving force (Pa)
$R$	gas constant ( $Pa m^3/(mol K)$ )
$Re$	Reynolds number
$Sc$	Schmidt number
$Sh$	Sherwood number
$\Delta t$	residence time of gas (s)
$T$	temperature (K)
$u_{inner}$	gas velocity in inner cylinder (m/s)
$u_G$	gas velocity (m/s)
$u_p$	droplet velocity (m/s)
$V_G$	gas flow rate ( $m^3/s$ )
$V_L$	slurry flow rate ( $m^3/s$ )
$V_R$	reactor volume ( $m^3$ )
$v_s$	superficial gas velocity
$w_c$	residual limestone mass (kg)
$w_g$	gypsum mass (kg)
$W_{out}$	water content in outlet flue gas ( $g/(kg \text{ dry-air})$ )
<b>Greek letters</b>	
$\rho_G$	gas density ( $kg/m^3$ )
$\rho_L$	liquid phase density ( $kg/m^3$ )
$\mu_G$	gas dynamics viscosity ( $kg/(m s)$ )
$\sigma$	surface tension of liquid (N/m)
$\xi$	molar ratio of $SO_2$ to limestone reagent (mol/mol)
$\eta$	$SO_2$ removal efficiency

cost and maintenance. (b) There are co-flows of gas and liquid in the preliminary treating chamber and no venturi structure in the inlet tube, therefore the pressure drop of the device is much lower than that of the original GWFDC. (c) The self-excitation chamber

has a second purification for the flue gas, which further improves the collection efficiency of the device. (d) Draft fans of the original GWFDC can be reused in the novel PCF device, reducing the investment cost of the PCF technology.

Control of the optimum operating parameters is one of the most effective ways to achieve a high removal efficiency of  $SO_2$  with the minimum operation cost. Therefore, the major objective of present study was to investigate the  $SO_2$  removal for PCF technology under different operating conditions including slurry pH and limestone content in feed stream,  $SO_2$  inlet concentration, liquid–gas ratio and superficial gas velocity. Experimental studies were carried out on a lab-scale PCF device, with the air– $SO_2$  mixture as simulated flue gas and  $CaCO_3$ -in-water suspension as absorbent. Meanwhile, the desulphurization process was to be analyzed using the two-film mass-transfer theory.

**2. Theoretical basis for  $SO_2$  absorption**

In wet FGD processes,  $SO_2$  diffuses through the gas phase to a liquid surface where it is dissolved and transferred by diffusion or convective mixing into the liquid phase. The  $SO_2$  transferring rate depends on a number of factors such as the solubility of  $SO_2$  in the liquid and its displacement from equilibrium. Some models have been proposed to describe this transfer across the phase boundary [7,8]. A well-known mass-transfer theory, the two-film theory, assumes that there are two thin stagnant films on either side of the gas–liquid interface, and, all the resistance to mass-transfer is contained in the two films. The absorption rate of  $SO_2$ ,  $N_{SO_2}$ , can be expressed as [9]

$$N_{SO_2} = K_G a \Delta p_{SO_2} \tag{1}$$

where  $K_G$  is the total mass-transfer coefficient,  $a$  is the gas–liquid interface area,  $\Delta p_{SO_2}$  is the absorption driving force, determined by the following equation [10]:

$$\Delta p_{SO_2} = p_{SO_2,avg} - \frac{c_{SO_2}}{H_{SO_2}} \tag{2}$$

where  $H_{SO_2}$  is the Henry's constant of  $SO_2$ ,  $c_{SO_2}$  is the concentration of  $SO_2$  in liquid phase and  $p_{SO_2,avg}$  is the logarithmically averaged data measured for the variation of  $SO_2$  partial pressure in gas phase before and after absorption [11].

$$p_{SO_2,avg} = \frac{p_{SO_2,in} - p_{SO_2,out}}{\ln(p_{SO_2,in}/p_{SO_2,out})} \tag{3}$$

Let  $V_G$  and  $V_R$  are the gas flow rate and reactor volume, the time interval of gas–liquid contacting (or residence time of gas),  $\Delta t$ , is obtained by

$$\Delta t = \frac{V_R}{V_G} \tag{4}$$

Consequently, the gas–liquid interface area,  $a$ , is defined as [12]:

$$a = \frac{6V_L \Delta t}{d_p} \tag{5}$$

where  $V_L$  is the slurry flow rate and  $d_p$  is the average size of slurry droplets.

The total mass-transfer coefficient,  $K_G$ , in Eq. (1) is calculated by

$$\frac{1}{K_G} = \left( \frac{1}{k_G} + \frac{1}{EH_{SO_2}k_L} \right) \tag{6}$$

where  $k_G$  is the gas-side mass-transfer coefficient,  $k_L$  is the liquid-side mass-transfer coefficient and  $E$  is the mass-transfer enhancement factor. In limestone slurry,  $E$  can be calculated from

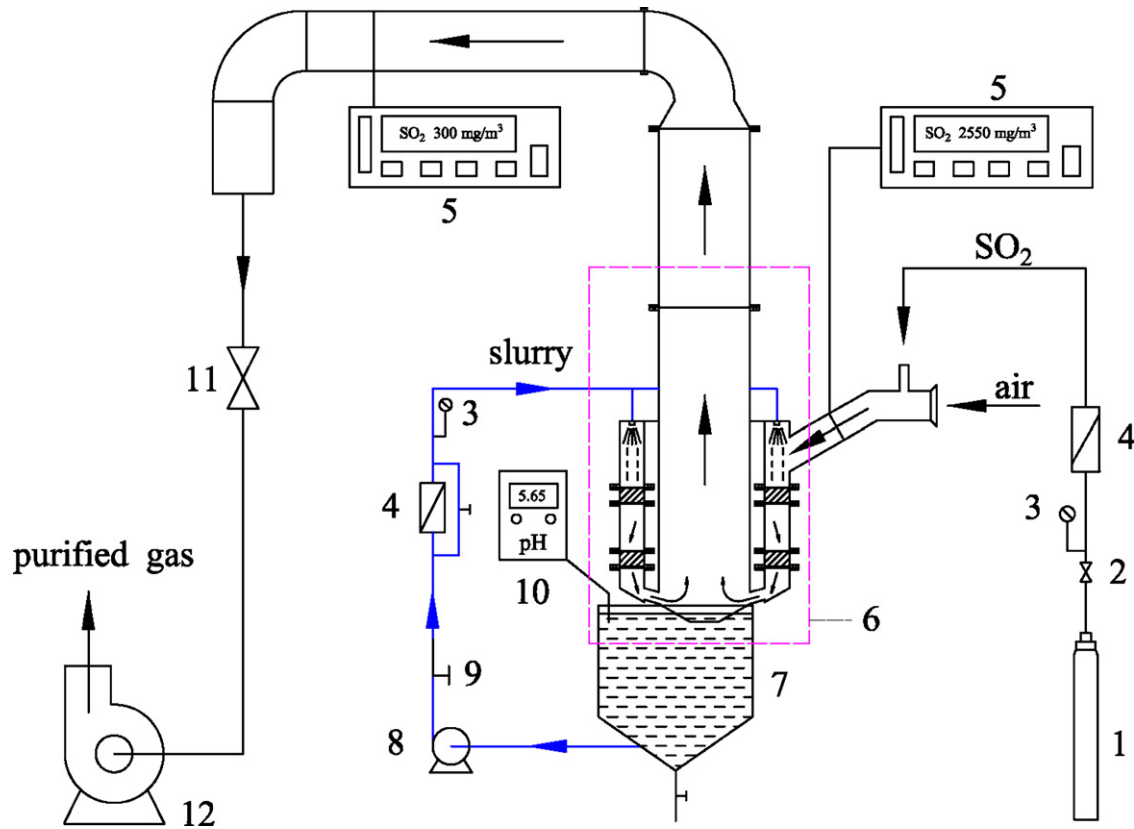


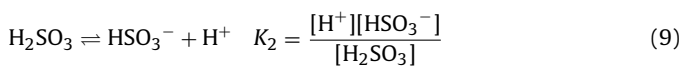
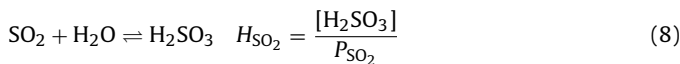
**Fig. 1.** Flow diagram of experimental setup for absorption of SO<sub>2</sub>: (1) bottled SO<sub>2</sub>, (2) pressure reduction valve, (3) manometer, (4) rotameter, (5) SO<sub>2</sub> analyzer, (6) PCF device (absorber), (7) slurry tank, (8) slurry pump, (9) valve, (10) pH meter, (11) volume damper, (12) exhaust fan.

the following equation [13,14]:

$$E = 1 + \xi \frac{D_{\text{CaCO}_3} \cdot c_{\text{CaCO}_3}}{D_L \cdot c_{\text{SO}_2}^*} \quad (7)$$

where  $D_{\text{CaCO}_3}$  is the diffusion coefficient of CaCO<sub>3</sub> in liquid phase,  $c_{\text{CaCO}_3}$  is the concentration of CaCO<sub>3</sub> in liquid phase,  $\xi$  is the molar ratio of SO<sub>2</sub> to limestone reagent,  $D_L$  is the diffusion coefficient of SO<sub>2</sub> in liquid phase and  $c_{\text{SO}_2}^*$  is the equilibrium concentration of SO<sub>2</sub> in liquid phase.

As described in the process, SO<sub>2</sub> is initially absorbed into the liquid and converted into H<sub>2</sub>SO<sub>3</sub>. A succession of equations between the SO<sub>2</sub> partial pressure in gas phase ( $P_{\text{SO}_2}$ ) and sulphite concentration in liquid phase can be considered [13–16]:



Thus, the total concentration of SO<sub>2</sub>,  $c_{\text{SO}_2}^*$ , in the liquid phase is equal to

$$c_{\text{SO}_2}^* = [\text{H}_2\text{SO}_3] + [\text{HSO}_3^-] + [\text{SO}_3^{2-}] \quad (11)$$

Substitution of the concentrations of H<sub>2</sub>SO<sub>3</sub>, HSO<sub>3</sub><sup>-</sup> and SO<sub>3</sub><sup>2-</sup> in Eq. (11) by the equilibrium constants for reactions (8)–(10) gives the following relationship:

$$c_{\text{SO}_2}^* = H_{\text{SO}_2} P_{\text{SO}_2} + \frac{H_{\text{SO}_2} P_{\text{SO}_2} K_2}{[\text{H}^+]} + \frac{H_{\text{SO}_2} P_{\text{SO}_2} K_2 K_3}{[\text{H}^+]^2} \quad (12)$$

### 3. Experimental

#### 3.1. Experimental setup and analytical methods

Research on the SO<sub>2</sub> removal from air was carried out in a specially designed system (Fig. 1), of which the essential element is the absorber (6) where SO<sub>2</sub> removal occurs. The desired amount of SO<sub>2</sub> in air was prepared by mixing bottled SO<sub>2</sub> (1) with air drafted by exhaust fan (12). Volumetric flow rates of SO<sub>2</sub> and air were adjusted by the pressure reduction valve (2) and volume damper (11), respectively. SO<sub>2</sub> was absorbed by limestone slurry. Limestone slurry prepared by mixing CaCO<sub>3</sub> of 25 μm with tap water was stored in slurry tank (7). The circulating pump (8) was provided for the recirculation of the slurry, and the quantity of the slurry pumped into the absorber was adjusted by means of a valve (9).

During the experiment, a digital pH meter (Model: HI 8424) (10) was employed to measure the pH value of slurry by inserting a pH probe into the liquid phase. Pitot tube (Model: Y25-150) was used to measure the gas flow rate, and two micro-computer smoke test instruments (Model: Leibo3020) (5) were employed to test SO<sub>2</sub> concentration in gas phase and water content in flue gas by putting sensors at the test cross sections of inlet tube and outlet tube simultaneously. Acid titration is the method to determine the amount of residual limestone in gypsum sample ( $w_c/w_g$ ).

#### 3.2. Absorber characteristics

The absorber used in this study is a lab-scale PCF device, as shown in Fig. 2. It consists of a preliminary treating chamber (4) and an inner cylinder (7). The air–SO<sub>2</sub> mixture first enters the preliminary treating chamber through the inlet tube (1) at the side-top of the absorber. The preliminary treating chamber is an annular

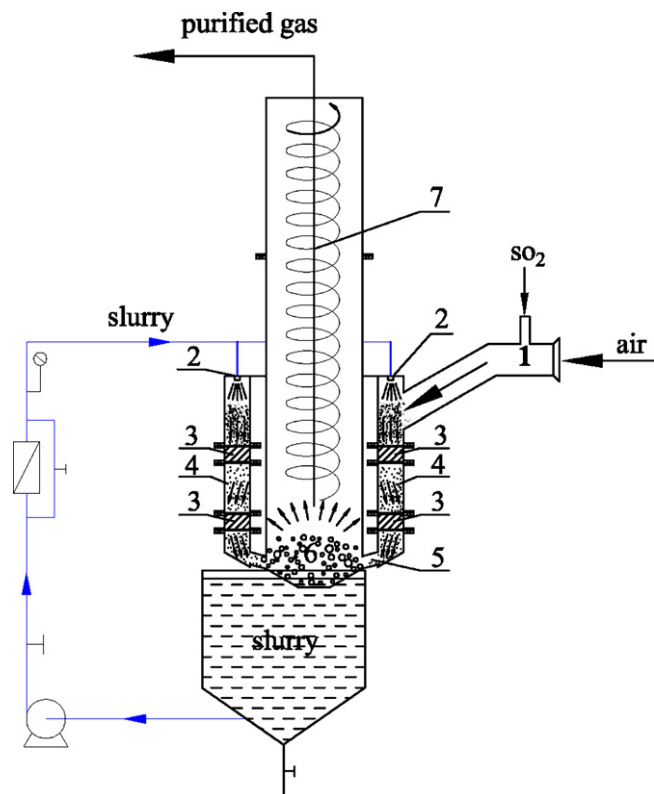


Fig. 2. PCF device as absorber: (1) inlet tube, (2) nozzle, (3) guide plate, (4) preliminary treating chamber, (5) self-excitation channel, (6) self-excitation chamber, (7) inner cylinder.

configuration with a width of 0.08 m and a height of 0.565 m. On the top of it, nozzles (2) are distributed and generate atomization. Thanks to the existence of guide plates (3), the absorbing liquid can form liquid film or curtain at or between the guide plates, and the gas–liquid turbulent intensity increases. When the gas passes through the preliminary treating chamber, SO<sub>2</sub> gets preliminary purification by reacting with CaCO<sub>3</sub> in the absorbing liquid. Then, the gas goes through the self-excitation channels (5) and enters the inner cylinder (7). The inner cylinder is a cylinder with a diameter of 0.3 m and a height of 1.5 m. At the bottom of it, there is a conical self-excitation chamber (6) where the rotary gas from self-excitation channels can impinge the liquid in slurry tank, and consequently lots of bubbles are produced, improving the secondary-purification effect for the gas. As the gas swirls up, water is removed from the air and the purified gas is released to the atmosphere through the exhaust tube. The scrubbed liquid flows into the inner cylinder along with self-excitation channels and returns to the recycle slurry tank.

### 3.3. Experimental procedure and basic conditions

The experiments were carried out in a batch mode. Before each run, the tank was refilled with fresh limestone slurry. The data were collected during the first 3–4 min. Because the slurry volume was about 450 L and the slurry pump capacity was equal to 100 L/min, the slurry was recycled only almost one time during 3–4 min runs. Thus SO<sub>2</sub> concentration in slurry did not increase significantly.

Table 1 gives the basic experimental conditions for the desulphurization system. With neglecting the variation of gas volume due to absorption, the SO<sub>2</sub> removal efficiency ( $\eta$ ) is defined as

$$\eta = \frac{c_{in} - c_{out}}{c_{in}} \times 100\% \quad (13)$$

Table 1  
Basic experimental conditions for the wet-type PCF desulphurization technology.

Parameter	Value
Temperature of gas	Atmosphere (25 ± 1 °C)
Operating pressure	Atmosphere
Gas flow rate (m <sup>3</sup> /s)	0.2402
Liquid–gas ratio (L/m <sup>3</sup> )	10
Droplet size (mm)	2.5
Limestone content in feed stream (wt%)	10
Limestone slurry pH	5.7 ± 0.1
SO <sub>2</sub> inlet concentration (g/m <sup>3</sup> )	2.5

Table 2  
Calculated mass-transfer coefficients for different droplet sizes.

dp (μm)	1500	2000	2500	3000
k <sub>G</sub> (mol/m <sup>2</sup> s Pa)	5.402 × 10 <sup>-5</sup>	4.591 × 10 <sup>-5</sup>	4.053 × 10 <sup>-5</sup>	3.664 × 10 <sup>-5</sup>
k <sub>L</sub> (m/s)	5.093 × 10 <sup>-4</sup>	4.104 × 10 <sup>-4</sup>	3.472 × 10 <sup>-4</sup>	3.028 × 10 <sup>-4</sup>
K <sub>G</sub> (mol/m <sup>2</sup> s Pa)	8.231 × 10 <sup>-6</sup>	6.686 × 10 <sup>-6</sup>	5.691 × 10 <sup>-6</sup>	4.988 × 10 <sup>-6</sup>

where  $c_{in}$  is the SO<sub>2</sub> inlet concentration and  $c_{out}$  is the SO<sub>2</sub> outlet concentration.

## 4. Results and discussion

### 4.1. Interpretation of mass-transfer coefficient

The mass-transfer between gas and liquid phases mainly takes place in the preliminary treating chamber of the PCF device, and as a consequence, the mass-transfer coefficients of this zone are interpreted in present study. Generally, the gas- and liquid-side mass-transfer coefficients can be measured by experiments. However, some correlations have been found to estimate the mass-transfer coefficients by means of the theory of diffusion with various conditions. In this study, the gas-side mass-transfer coefficient,  $k_G$ , was calculated from the Frossling correlation [17]:

$$Sh = \frac{k_G d_p RTP_{Bm}}{D_G P_T} = 2 + 0.6 Re^{1/2} Sc^{1/3} \quad (14)$$

where  $P_{Bm}$  is logarithmically averaged pressure of interface and gas-phase of inert component,  $P_T$  is the overall pressure,  $D_G$  is the diffusion coefficient of SO<sub>2</sub> in gas phase,  $Sh$ ,  $Re$  and  $Sc$  are the Sherwood number, Reynolds number and Schmidt number, respectively;  $Re$  is calculated by Eq. (15) and  $Sc$  is calculated by Eq. (16).

$$Re = \frac{\rho_G d_p |u_G - u_p|}{\mu_G} \quad (15)$$

$$Sc = \frac{\mu_G}{\rho_G D_G} \quad (16)$$

where  $\rho_G$ ,  $u_G$  and  $\mu_G$  are the gas density, velocity and dynamics viscosity, respectively;  $u_p$  is the average velocity of slurry droplets.

The liquid-side mass-transfer coefficient,  $k_L$ , is estimated by [17]:

$$k_L = 0.88 \sqrt{\sqrt{\frac{8\sigma}{3\pi m_p}} D_L} \quad (17)$$

where  $\sigma$  is the surface tension of liquid and  $m_p$  is the mass of a droplet.

Table 2 shows the effect of droplet size on the mass-transfer coefficients of SO<sub>2</sub> in preliminary treating chamber, with both the gas- and liquid-side mass-transfer coefficients gradually decreasing with increasing droplet size. Provided that the gas- and liquid-side mass-transfer resistances are defined as  $1/k_G$  and  $1/(H_{SO_2} E k_L)$ , respectively, the estimation of which phase controls the mass-transfer can be ascribed to the ratio of gas-side resistance to the total mass-transfer resistance,  $(1/k_G)/(1/K_G)$ . If  $1/k_G$

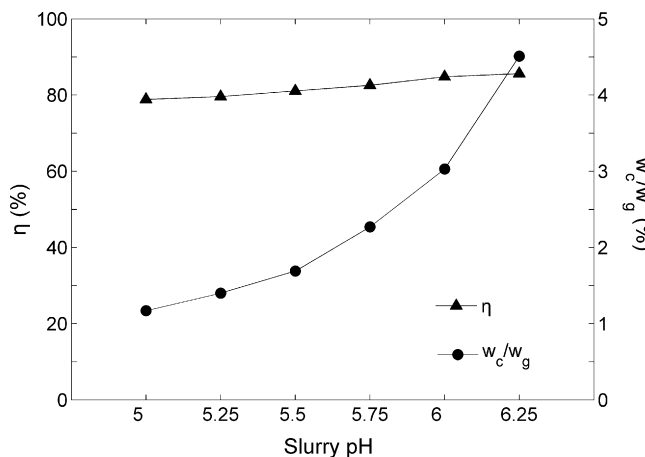


Fig. 3. Relationship of  $\eta$ ,  $w_c/w_g$  and slurry pH.

is nearly equal to  $1/K_G$ , the mass-transfer is gas phase control and a ratio of  $(1/k_G)/(1/K_G) \leq 0.1$  is the criterion for liquid phase control [13]. According to Table 2, it can be calculated that the ratios of  $(1/k_G)/(1/K_G)$  are 0.1524, 0.1457, 0.1404 and 0.1362 for droplet sizes of 1500, 2000, 2500 and 3000  $\mu\text{m}$ , respectively, indicating that both gas- and liquid-side resistances are important, with the absorption rate likely to be controlled by a combination of gas- and liquid-film diffusion controls. The reduction in either side resistance can result in an increasing of  $\text{SO}_2$  removal. On the other hand, the calculations show that the ratio of  $(1/k_G)/(1/K_G)$  is slightly bigger than 0.1, which also can be concluded that the absorption of  $\text{SO}_2$  into the limestone slurry to a large extent is liquid-side controlled. The conclusion agrees with that of Brogren and Karlsson [6].

#### 4.2. Influence of slurry pH and limestone concentration

Apart from the  $\text{SO}_2$  removal efficiency, another essential parameter in the operation of a wet FGD plant based on limestone-gypsum is the amount of residual limestone in the gypsum because of a good utilization of limestone and a saleable gypsum product of less than 3 wt.% residual limestone [13]. And hence, an experiment was first carried out to test the influence of slurry pH on  $\text{SO}_2$  removal efficiency ( $\eta$ ) and residual limestone content in the gypsum ( $w_c/w_g$ ). The results are shown in Fig. 3.

When the slurry pH values increase from 5.0 to 6.25, the  $\text{SO}_2$  removal efficiency appears to increase almost linearly from 78.8% to 85.6%. This is because at higher pH values, the dissociation reaction of  $\text{SO}_2$ :



is shifted to the right, leading to an increase in the enhancement factor defined by Eq. (7) and thereby in the degree of desulphurization [18]. But during the course, the prevailing sulfurous species is sulphite ion ( $\text{SO}_3^{2-}$ ) as opposed to bisulphite ( $\text{HSO}_3^-$ ).  $\text{SO}_3^{2-}$  is more difficultly oxidized to  $\text{SO}_4^{2-}$  than  $\text{HSO}_3^-$  [19]. The  $\text{CaSO}_3$  easily crystallizes on the limestone surface, which prevents  $\text{SO}_2$  further absorption and reaction with  $\text{CaCO}_3$ . At the same time, higher pH values hinder the dissolution of limestone. The fact that the residual limestone content in the gypsum increases with slurry pH increasing in Fig. 3 reflects those phenomena. And in addition, the operation at lower pH ranges also has a smaller risk of scaling and plugging [20]. Thus, it is advantageous to run a wet FGD plant at lower value of pH from limestone utilization and gypsum production point of views. However,  $\text{SO}_2$  removal efficiency decreases at lower pH. Therefore, the normal operating condition should be controlled at pH of about 5.7 for the process.

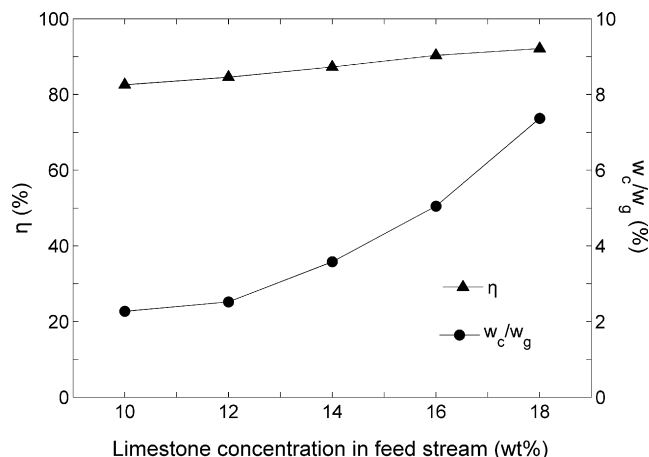


Fig. 4. Relationship of  $\eta$ ,  $w_c/w_g$  and limestone concentration in feed stream.

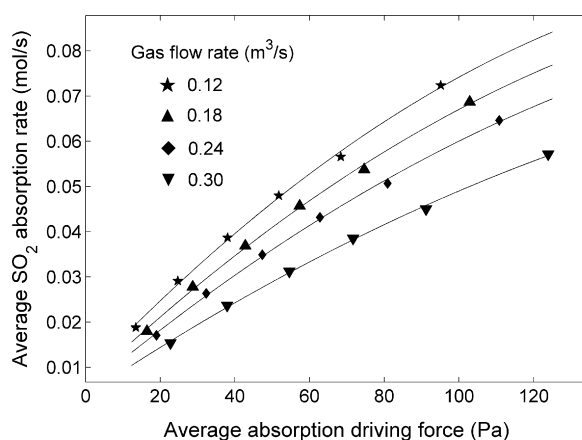


Fig. 5. Average absorption rate for different absorption driving forces.

Fig. 4 illustrates the relationship of  $\text{SO}_2$  removal efficiency ( $\eta$ ), residual limestone content in the gypsum ( $w_c/w_g$ ) and limestone concentration in feed stream. The results show that  $\text{SO}_2$  removal efficiency increases with limestone concentration increasing, and it is 82.56% at the limestone concentration of 10 wt.% and increases to 92.14% at the limestone concentration of 18 wt.%. The larger molar Ca/S caused by higher limestone concentrations in slurry accounts for this trend. As to the residual limestone content in the gypsum, it also increases with limestone concentration in feed stream increasing. And hence, the reasonable limestone concentration determined should consider from those two aspects of  $\eta$  and  $w_c/w_g$ . In present study, when the limestone concentration is chosen as 13 wt.%,  $w_c/w_g$  is less than 3% and  $\eta$  can reach 85.5%, meeting the requirements of utilization of limestone and environmental protection.

#### 4.3. Influence of $\text{SO}_2$ concentration

Fig. 5 presents the relationship between the average absorption rate and absorption driving force defined by Eq. (2) at different gas flow rates. As shown in this figure that the experimental points, in the range of gas flow rates from 0.12 to 0.30  $\text{m}^3/\text{s}$ , can be described by a quadratic equation, and the average absorption rate decreases with gas flow rate increasing. These results are somewhat different from those of Bokotko et al. [11] and Wu et al. [12], who reported the absorption rate was in direct portion to the driving force and could be described by linear functions. Likely, this difference is resulted from different operation conditions. In this study, the slurry flow

**Table 3**  
Comparison of absorption rate of PCF device, ASH [11] and impinge stream scrubber [21].

Absorption driving force (Pa)	Absorption rate (mol/s)		
	PCF device	ASH	Impinge stream scrubber
24.72	0.029	$0.094 \times 10^{-3}$	0.012
51.76	0.048	$0.188 \times 10^{-3}$	0.019
68.40	0.056	$0.263 \times 10^{-3}$	0.024

rate is fixed. The increase in gas flow rate incites the decrease in gas-side mass-transfer coefficient and liquid–gas ratio, reducing the average absorption rate. Meanwhile, the variations in absorption driving force are obtained by changing SO<sub>2</sub> inlet concentrations. These measures change the total mass-transfer coefficient, and consequently nonlinear relationship of average absorption rate and average absorption driving force is formed, in accordance with the Eq. (1). Furthermore, the average absorption rate of the PCF device is bigger than that of other absorbers described in [11,21] due to the existence of guide plates and second-purification of self-excitation chamber for the gas. The detailed comparison is shown in Table 3.

Fig. 6 gives the results of SO<sub>2</sub> removal efficiency ( $\eta$ ) at various gas flow rate for different SO<sub>2</sub> inlet concentrations ( $c_{in}$ ). The curves in diagram show that for constant gas flow rate an increase of  $c_{in}$  leads to a decrease in  $\eta$ . As the inlet concentration of SO<sub>2</sub> varies from 1.254 to 5.634 g/m<sup>3</sup>, each of  $\eta$  decreases about 13%. But this does not imply decrease in SO<sub>2</sub> absorption rate, and on the contrary, the absorption rate is a simple increasing function of  $c_{in}$ , as seen in Fig. 5. The decreasing tendency of  $\eta$  is only due to faster increase in the amount of SO<sub>2</sub> than that needs to be absorbed [12]. And hence in the case of very high  $c_{in}$ , certain improvement of operating conditions, i.e., increasing liquid–gas ratio, is needed to achieve higher desulphurization efficiency. On the other hand, for constant SO<sub>2</sub> inlet concentration,  $\eta$  decreases as the gas flow rate increases. The possible reason is that the gas-side mass-transfer coefficient, residence time of gas in the absorber and liquid–gas ratio become shorter as the gas flow rate is enhanced, and meanwhile, larger gas flow rate means smaller molar ratio of Ca/S.

4.4. Influence of gas–liquid ratio

From the economic point of view, the liquid–gas ratio,  $V_L/V_G$ , has been found to be one of the most important criterions for reporting the absorber performance [22]. In practical FGD processes, the  $V_L/V_G$  value can be calculated according to its minimum value,

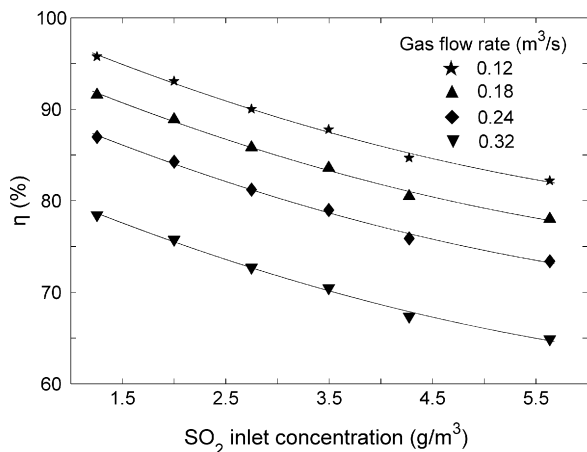


**Fig. 6.** SO<sub>2</sub> removal efficiency at various gas flow rate for different SO<sub>2</sub> inlet concentrations.

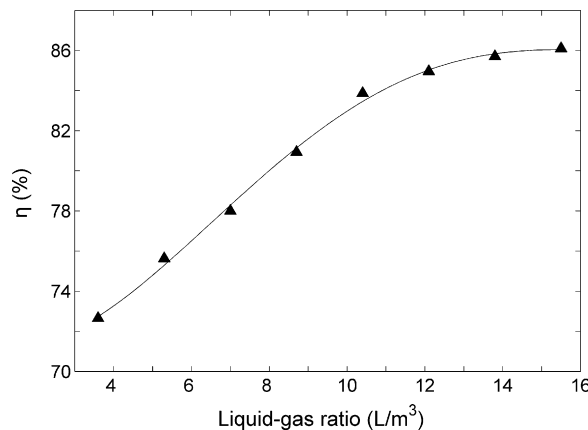


**Fig. 7.** Relationship between  $\eta$  and liquid–gas ratio.

expressed as:

$$\frac{V_L}{V_G} = (1.1-2.0) \left( \frac{V_L}{V_G} \right)_{\min} \tag{19}$$

where

$$\left( \frac{V_L}{V_G} \right)_{\min} = \frac{(P_{SO_2, in} - P_{SO_2, out})}{(c_{SO_2}^* - c_{SO_2})} \cdot \frac{\rho_L}{(P - P_{SO_2, in})M_M} \tag{20}$$

where  $\rho_L$  is the liquid phase density,  $P$  is the atmospheric pressure and  $M_M$  is the molar mass of the liquid phase.

For the PCF device, the value of  $(V_L/V_G)_{\min}$  was calculated as 7.2 L/m<sup>3</sup>. The experiments were carried out at a fixed gas flow rate and liquid flow rate was controlled according to the requested  $V_L/V_G$ . The relationship between SO<sub>2</sub> removal efficiency and liquid–gas ratio is shown in Fig. 7.

From Fig. 7, it can be seen that the SO<sub>2</sub> removal efficiency increases continuously with  $V_L/V_G$  increasing in the range of  $V_L/V_G < 11$  L/m<sup>3</sup>. However, when  $V_L/V_G$  is more than 11 L/m<sup>3</sup>, the curve in the diagram increases relaxed. The reason can be explained as follows: With an increase in the amount of  $V_L/V_G$  delivered to the absorber, the gas–liquid interface area defined by Eq. (5) and total alkalinity for the absorption of SO<sub>2</sub> increase when the gas flow rate is fixed. Consequently, the SO<sub>2</sub> absorption rate increases, and removal efficiency of SO<sub>2</sub> is enhanced. However, when  $V_L/V_G$  is too large, the cohesion of droplets will strengthen, and the effective gas–liquid interface area no longer increases but even decreases, resulting in smaller mass-transfer coefficient [12]. This moment, further increase in  $V_L/V_G$  becomes meaningless, and the average absorption rate and removal efficiency of SO<sub>2</sub> increase relaxed. In present study, the SO<sub>2</sub> outlet concentration obtained in the range of  $V_L/V_G$  of 8.7–10.4 L/m<sup>3</sup> is low enough from the point of meeting the emission standard of air pollutants for coal-burning boiler [23]. And hence, this range can be considered to be optimal.

4.5. Influence of superficial gas velocity

Superficial gas velocity is an important operating parameter in FGD process because it affects the removal of SO<sub>2</sub> and H<sub>2</sub>O from air, and the pressure drop ( $\Delta p$ ) in absorber. The relationship between SO<sub>2</sub> removal efficiency ( $\eta$ ) and gas velocity has been studied in Section 4.3,  $\eta$  decreasing with the gas velocity increase. The aim of this section is to investigate the relationship between pressure drop and superficial gas velocity. The results are given in Fig. 8. Here, superficial gas velocity is the velocity of gas in preliminary treating chamber, and the liquid–gas ratio is fixed.

As shown in Fig. 8,  $\Delta p$  increases proportionally with superficial gas velocity increasing. Their relationship can be described with

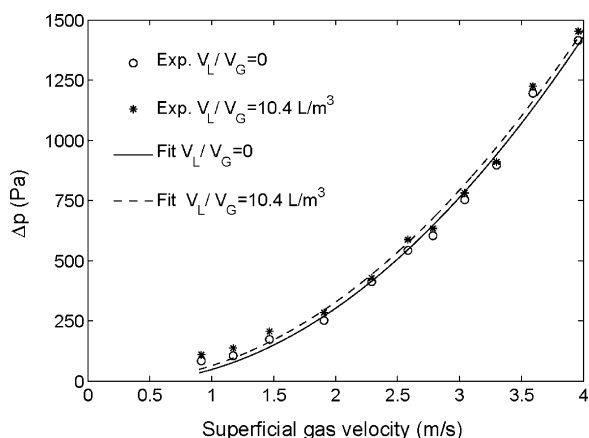


Fig. 8. Relationship between  $\Delta p$  and superficial gas velocity.

a good approximation by quadratic functions ( $v_s$  – superficial gas velocity):

$$\frac{V_L}{V_G} = 0, \quad \Delta p = 103.1v_s^2 - 54.83v_s, \quad R^2 = 0.9931 \quad (21)$$

$$\frac{V_L}{V_G} = 10.4 \text{ L/m}^3, \quad \Delta p = 100.2v_s^2 - 36.07v_s, \quad R^2 = 0.9900 \quad (22)$$

Meanwhile, some other information can be observed from the figure: (a) The influence of liquid–gas ratio on  $\Delta p$  is negligible, while that of superficial gas velocity is quite heavy. When the liquid–gas ratio increases from 0 to 10.4 L/m<sup>3</sup>, the average difference of  $\Delta p$  is only about 50 Pa. And superficial gas velocity increases from 0.92 to 3.96 m/s,  $\Delta p$  increases about 1300 Pa. (b) Generally speaking,  $\Delta p$  over the PCF device is relative small by comparison with that of the other absorbers reported previously [24–26]. When the superficial gas velocity reaches 3.5 m/s (5.97 m/s in inner cylinder), the pressure drop of the PCF device is only 1200 Pa around; while that of other absorbers is high up to 1500 Pa and even higher. Low pressure drop for the PCF device is due to co-flows in the preliminary treating chamber and no venturi structure in the inlet tube. Certain statistics indicated that the increase of  $\Delta p$  in the absorber caused the increase of energy consumption [27]. Thus, on the premise of the same treatment volume,  $\Delta p$  in the absorber should be minimized. The results indicate that under the same pressure drop the PCF device possesses a larger specific capacity for flue gas treatment.

#### 4.6. Dewatering performance

It is well known that the flue gas scrubbed by the absorbent liquid will contain some water. When the content of water in flue gas is much higher, the water will cause the pipes to corrode and destroy the draft fans. Therefore, the flue gas dewatering is an important part of wet FGD. As for the spraying tower, the main influence factors on water content in flue gas are the liquid–gas ratio and gas velocity. In this section, the relationship of water content in outlet flue gas ( $W_{out}$ ), liquid–gas ratio and gas velocity in inner cylinder ( $u_{inner}$ ) was discussed for the PCF device, as shown in Fig. 9.

From Fig. 9(a), it can be seen that the water content in outlet flue gas is almost kept a constant when the liquid–gas ratio is changed from 4.09 to 12.8 L/m<sup>3</sup>, and the highest value of  $W_{out}$  is not more than 22 g/(kg dry-air). When the liquid–gas ratio is fixed, as shown in Fig. 9(b), the water content in outlet flue gas is decreased slightly. The reason may be that the centrifugal force is increased as the gas velocity in inner cylinder increases, which improves the dewatering ability of inner cylinder. Combining the results of Fig. 9, it can be concluded that the PCF device possesses a good dewatering performance. The fact that no water was observed in outlet flue gas

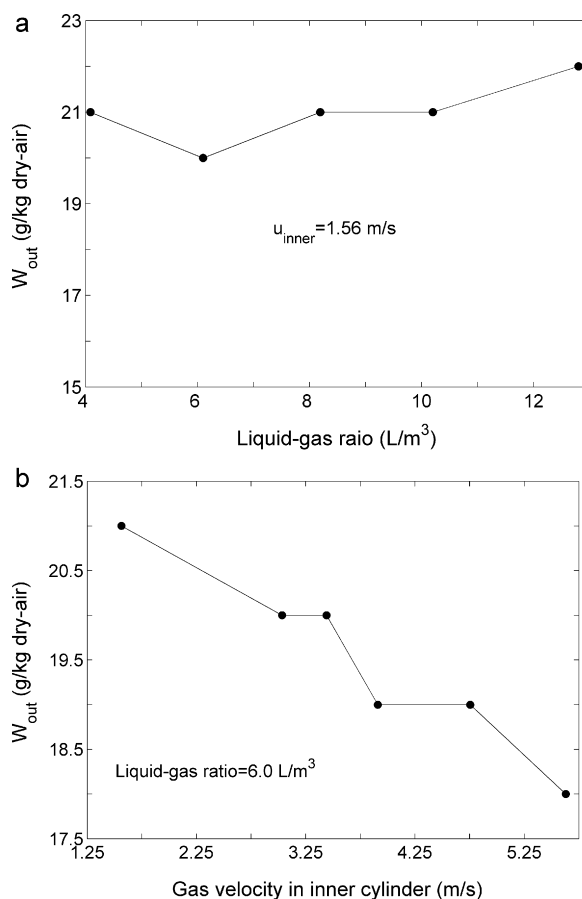


Fig. 9. Relationship of water content in outlet flue gas, liquid–gas ratio and gas velocity in inner cylinder.

during the experiments testifies this point once more. Therefore, the demister is out of consideration in the PCF device, reducing the energy-consumption, cost and maintenance.

#### 5. Conclusions

The experimental investigation with a lab-scale PCF device initially developed for wet flue gas desulphurization show that the device has low pressure drop, large specific capacity for flue gas treatment, high absorption rate and good dewatering performance. Under the moderate conditions employed, the concentration of SO<sub>2</sub> in outlet flue gas can achieve a much lower level than that of permitted. During the course, some reasonable operating parameters were obtained including the pH value of 5.7 ± 0.1, the limestone concentration in feed stream of 13 wt.%, SO<sub>2</sub> inlet concentration of below 4.1 g/m<sup>3</sup>, liquid–gas ratio of 8.7–10.4 L/m<sup>3</sup> and superficial gas velocity in preliminary treating chamber of 2.0–2.5 m/s (3.4–4.3 m/s in inner cylinder). Meanwhile, the desulphurization process was analyzed using the two-film theory of gas–liquid, which indicated that the SO<sub>2</sub> removal rate was controlled by a combination of both gas- and liquid-film diffusions in the range of operating tested conditions. According to those results, it is believed that the PCF device will exhibit a promising future in the field of wet FGD.

#### Acknowledgements

The authors gratefully acknowledge the financial support of the National Natural Science Foundation Project of China (Nos. NSFC-50878080 and NSFC-50978088) and the Key Scientific and Technological Special Project of Changsha City in China (No. K0902006-31).

## References

- [1] L. Marocco, F. Inzoli, Multiphase Euler-Lagrange CFD simulation applied to wet flue gas desulphurization technology, *Int. J. Multiphase Flow* 35 (2009) 185–194.
- [2] B.L. Dou, Y.C. Byun, J.G. Hwang, Flue gas desulphurization with an electrostatic spraying absorber, *Energy Fuel* 22 (2008) 1041–1045.
- [3] Ü.T. Ün, A.S. Kopalal, Ü.B. Ögütveren, Sulfur dioxide removal from flue gases by electrochemical absorption, *Sep. Purif. Technol.* 53 (2007) 57–63.
- [4] A. Gómez, N. Fueyo, A. Tomás, Detailed modeling of a flue-gas desulfurization plant, *Comput. Chem. Eng.* 31 (2007) 1419–1431.
- [5] F.J. Gutierrez Ortiz, F. Vidal, P. Ollero, L. Salvador, V. Cortes, A. Gimenez, Pilot-plant technical assessment of wet flue gas desulfurization using limestone, *Ind. Eng. Chem. Res.* 45 (2006) 1466–1477.
- [6] C. Brogren, H.T. Karlsson, Modeling the absorption of SO<sub>2</sub> in a spray scrubber using the penetration theory, *Chem. Eng. Sci.* 52 (1997) 3085–3099.
- [7] W.R. Vieth, J.H. Porter, T.K. Sherwood, Mass transfer and chemical reaction in a turbulent boundary layer, *Ind. Eng. Chem. Fundam.* 2 (1963) 1–3.
- [8] P.V. Danckwerts, Significance of liquid-film coefficients in gas absorption, *Ind. Eng. Chem. Res.* 43 (1951) 1460–1467.
- [9] M. Gerbec, A. Stergaršek, R. Kocjancic, Simulation model of wet flue gas desulphurization plant, *Comput. Chem. Eng.* 19 (1995) s283–s286.
- [10] A. Lancia, D. Musmarra, F. Pepe, Modeling of SO<sub>2</sub> Absorption into limestone suspension, *Ind. Eng. Chem. Res.* 36 (1997) 197–203.
- [11] R.P. Bokotko, J. Hupka, J.D. Miller, Flue gas treatment for SO<sub>2</sub> removal with air-sparged hydrocyclone technology, *Environ. Sci. Technol.* 39 (2005) 1184–1189.
- [12] Y. Wu, Q. Li, F. Li, Desulfurization in the gas-continuous impinging stream gas-liquid reactor, *Chem. Eng. Sci.* 62 (2007) 1814–1824.
- [13] B.L. Dou, W.G. Pan, Q. Jin, W.H. Wang, Y. Li, Prediction of SO<sub>2</sub> removal efficiency for wet flue gas desulfurization, *Energy Convers. Manage.* 50 (2009) 2547–2553.
- [14] C. Lin, J.Y. Zhang, Enhancement Factor of Gas Absorption in Gas-Liquid-Solid Three-Phase Reaction System Accompanied by Solid Dissolution [C]//Advances in Separation Science and Technology, China Environmental Science Press, Beijing, 1998, pp. 606–610.
- [15] G. Vázquez, G. Antorrena, F. Chenol, F. Paleo, Absorption of SO<sub>2</sub> by aqueous NaOH solutions in the presence of a surfactant, *Chem. Eng. Technol.* 11 (1988) 156–162.
- [16] Z.G. Tang, C.C. Zhou, C. Chen, Studies on flue gas desulphurization by chemical absorption using an ethylenediamine-phosphoric acid solution, *Ind. Eng. Chem. Res.* 43 (2004) 6714–6722.
- [17] J. Warych, M. Szymanowski, Model of the wet limestone flue gas desulfurization process for cost optimization, *Ind. Eng. Chem. Res.* 40 (2001) 2597–2605.
- [18] Y.J. Zheng, S. Kiil, J.E. Johnsson, Experimental investigation of a pilot-scale jet bubbling reactor for wet flue gas desulphurization, *Chem. Eng. Sci.* 58 (2003) 4695–4703.
- [19] M. Takeshita, H. Soud, FGD Performance and Experience on Coal-Fired Plant, IEACR/58, IEA Coal Research, London, 1993.
- [20] D.P. Burford, I.G. Pearl, G.E. Stevens, Phase I results from the DOE/SCS CT-121 project at Georgia Power's Plant Yates, in: Proceedings of 56th American Power Conference, vol. 2, Chicago, IL, 1994, pp. 1655–1660.
- [21] F. Cheng, Experimental and theoretical study on impinge stream scrubber wet flue gas desulfurization, Ph.D. Dissertation, University of Zhejiang, Hangzhou, 2005 (in Chinese).
- [22] I. Hrastel, M. Gerbec, A. Stergaršek, Technology optimization of wet flue gas desulphurization process, *Chem. Eng. Technol.* 30 (2007) 220–233.
- [23] Chinese National Environmental Protection Ministry, Emission standard of air pollutants for coal-burning oil-burning gas-fired boiler (GWBP3-1999), China, 1999.
- [24] R.H. Boll, Particle Collection and pressure drop in venturi scrubbers, *Ind. Eng. Chem. Fundam.* 12 (1973) 40–50.
- [25] G. Tosun, A study of concurrent downflow of nonfoaming gas-liquid systems in a packed bed. 2. Pressure drop: search for a correlation, *Ind. Eng. Chem. Proc. Des. Dev.* 23 (1984) 35–39.
- [26] B.N. Thorat, K. Kataria, A.V. Kulkarni, J.B. Joshi, Pressure drop studies in bubble columns, *Ind. Eng. Chem. Res.* 40 (2001) 3675–3688.
- [27] B.C. Meikap, M.N. Biswas, Fly-ash removal efficiency in a modified multistage bubble column scrubber, *Sep. Purif. Technol.* 36 (2004) 177–190.